Journal of Solid State Chemistry **165,** 303–311 (2002)
doi:10.1006/jssc.2002.9534, available online at http://www.idealibrary.com on IDEAL®

^{6}Li and ^{7}Li MAS NMR Studies on Fast Ionic Conducting Spinel-Type Li_2MgCl_4, $Li_{2-x}Cu_xMgCl_4$, $Li_{2-x}Na_xMgCl_4$, and Li_2ZnCl_4

R. Nagel,* Th. W. Groß,† H. Günther,† and H. D. Lutz*,[1]

*Anorganische Chemie I, Universität-GH Siegen, 57068 Siegen, Germany; and †Organische Chemie II, Universität-GH Siegen, 57068 Siegen, Germany

Received July 7, 2001; in revised form January 23, 2002; accepted February 8, 2002

DEDICATED TO PROFESSOR DR. MARIANNE BAUDLER ON THE OCCASION OF HER 80TH BIRTHDAY

^{6}Li and ^{7}Li MAS NMR spectra including 1D-EXSY (exchange spectroscopy) and inversion recovery experiments of fast ionic conducting Li_2MgCl_4, $Li_{2-x}Cu_xMgCl_4$, $Li_{2-x}Na_xMgCl_4$, and Li_2ZnCl_4 have been recorded and discussed with respect to the dynamics and local structure of the lithium ions. The chemical shifts, intensities, and half-widths of the Li MAS NMR signals of the inverse spinel-type solid solutions $Li_{2-x}M^I_xMgCl_4$ (M^I = Cu, Na) with the copper ions solely at tetrahedral sites and sodium ions at octahedral sites and the normal spinel-type zinc compound, respectively, confirm the assignment of the low-field signal to Li^{tet} of inverse spinel-type Li_2MgCl_4 and the high-field signal to Li^{oct} as proposed by Nagel *et al.* (2000). In contrast to spinel-type $Li_{2-2x}Mg_{1+x}Cl_4$ solid solutions with clustering of the vacancies and Mg^{2+} ions, the Cu^+ and Na^+ ions are randomly distributed on the tetrahedral and octahedral sites, respectively. The activation energies due to the various dynamic processes of the lithium ions in inverse spinel-type chlorides obtained by the NMR experiments are $E_a = 6.6–6.9$ and $\Delta G^* > 79$ kJ mol^{-1} (in addition to 23, 29, and 75 kJ mol^{-1} obtained by other techniques), respectively. The largest activation energy of >79 kJ mol^{-1} corresponds to hopping exchange processes of Li ions between the tetrahedral 8*a* sites and the octahedral 16*d* sites. The smallest value of 6.6–6.9 kJ mol^{-1}, which was derived from the temperature dependence of both the spin-lattice relaxation times T_1 and the correlation times τ_C of Li^{tet}, reveals a dynamic process for the Li^{tet} ions inside the tetrahedral voids of the structure, probably between fourfold 32*e* split sites around the tetrahedral 8*a* site. © 2002 Elsevier Science (USA)

Key Words: **^{6}Li and ^{7}Li MAS NMR spectra; 1D-EXSY and inversion recovery experiments; spinel-type quaternary lithium magnesium chlorides; local structure; dynamics; and activation energies of lithium ions.**

INTRODUCTION

Ternary lithium chlorides $Li_2M^{II}Cl_4$ (M^{II} = Mg, Mn, and Cd) belong to the best lithium ion conductors known so far (1–4). They crystallize at room temperature in an inverse spinel-type structure (space group $Fd\bar{3}m$) with the lithium ions on the tetrahedral 8*a* sites and the octahedral 16*d* sites and random distribution of M^{II} and Li on the octahedral site. The mechanism of the ionic conductance can be described as interstitial diffusion of tetrahedral coordinated lithium ions via empty octahedral interstitial 16*c* sites (2, 3). The ionic conductivity of these compounds strongly increases with increasing temperature. This is caused by an increasing disorder of the tetrahedral coordinated Li^+ ions to interstitial octahedral 16*c* sites (2, 5). On the other hand, the electric conductivity of Li_2ZnCl_4, which crystallizes in a normal spinel-type structure with only octahedrally coordinated Li^+ ions (6), is about two orders of magnitude smaller than that of the above-mentioned $Li_2M^{II}Cl_4$ compounds (3).

Very recently, we performed ^{6}Li and ^{7}Li MAS NMR experiments on Li_2ZnCl_4 and Li_2MgCl_4 including $Li_{2-2x}Mg_{1+x}Cl_4$ solid solutions (7, 8). The latter display an increased ionic conductivity compared to stoichiometric Li_2MgCl_4 (9, 10). In the case of the inverse spinel-type compounds, two NMR signals have been observed, viz., at δ 1.2 and 0.3 ppm rel. to ^{6}LiCl, whereas for normal spinel-type Li_2ZnCl_4, as expected, only one signal at 0.2 ppm was recorded. The different chemical shifts and half-widths were ascribed to different shielding and to dipolar interactions. The changes observed for these parameters with increasing Mg content were explained by assuming the formation of vacancies at the tetrahedral sites through substitution of Li by Mg and through clustering of the randomly distributed Li^+ and Mg^{2+} ions at the octahedral sites.

Because in the preceding paper (8) some questions arose with respect to the assignment of the two NMR signals in the case of inverse spinel-type chlorides, we performed new ^{6}Li and ^{7}Li MAS NMR studies on ^{6}Li-enriched spinel-type $Li_{2-x}Na_xMgCl_4$ and $Li_{2-x}Cu_xMgCl_4$ solid solutions (11, 12). In the case of these compounds, the relative intensities of the ^{6}Li NMR signals for the tetrahedral and octahedral sites should be affected in an opposite manner

[1]To whom correspondence should be addressed.

0022-4596/02 $35.00

depending on the respective occupation factors. As was already established by neutron diffraction experiments (12–14), Na^+ ions exclusively replace octahedral coordinated Li^+ ions whereas Cu^+ ions substitute only tetrahedral coordinated Li^+ sites. In order to study the strongly increasing disorder of the lithium ions in inverse spinel-type chlorides at elevated temperatures and the dynamics of these ions, we also performed high-temperature ^{6}Li MAS NMR experiments on $Li_{2-x}Cu_xMgCl_4$ solid solutions, relaxation time measurements on both $^6Li_2ZnCl_4$ and $^6Li_2MgCl_4$, and 1D-EXSY studies for $^6Li_2MgCl_4$. Additional information is given in (11, 12).

EXPERIMENTAL

Polycrystalline samples of Li_2ZnCl_4 and Li_2MgCl_4, and $Li_{2-x}Cu_xMgCl_4$, and $Li_{2-x}Na_xMgCl_4$ solid solutions were prepared by fusing stoichiometric amounts of anhydrous binary chlorides in evacuated sealed borosilicate tubes and subsequent annealing at 573 K for about 6 weeks (12). The starting materials were LiCl (enriched to 95% ^{6}Li), NaCl, CuCl, $MgCl_2$, and $ZnCl_2$. LiCl was obtained by neutralizing the respective ^{6}Li-enriched $LiOH \cdot H_2O$ solutions with HCl, evaporating H_2O, and heating the precipitate at 573 K in vacuum. For $MgCl_2$, $ZnCl_2$, NaCl, and CuCl, $MgCl_2 \cdot 6H_2O$ and commercial anhydrous $ZnCl_2$, NaCl, and CuCl were dehydrated and dried in an HCl stream at 773 K ($MgCl_2 \cdot 6H_2O$) and 573 K, respectively. Since most compounds are sensitive to air and moisture, they must be handled in a glove box under argon atmosphere. All samples were characterized by X-ray Guinier powder photographs (Huber Guinier 600 system) using Cu$K\alpha_1$ radiation.

The ^{6}Li and ^{7}Li MAS NMR spectra were measured with a Bruker MSL 300 spectrometer, controlled by the DISMSL software (15) and operating at a magnetic field strength of 7 T which corresponds to resonance frequencies of 44.17 MHz for ^{6}Li and 116.59 MHz for ^{7}Li, respectively. The 90° pulse width ranged from 2 to 6 μs.

For the measurements, powdered samples (200 mg each) were filled in ZrO_2 rotors, which were sealed by Kel-F caps. A 4 mm double probe with double bearing system was used as sample holder. Adjustment of the spinning rate (and the temperature in the case of the temperature-dependent measurements) was established by a B-VT 2000-MAS remote control unit. The spinning rates of the MAS NMR experiments were 10 kHz, those for the SLOW MAS NMR spectra 507 (^{6}Li) and 1201 Hz (^{7}Li), respectively. Natural and ^{6}Li-enriched LiCl served as reference.

1D-EXSY (Exchange spectroscopy) experiments (16) on the low-field signal (Li^{tet}) of $^6Li_2MgCl_4$ were performed in order to determine the longitudinal relaxation time T_1 of this signal and the rate constant for chemical exchange. T_1 measurements for ^{6}Li in Li_2ZnCl_4 were carried out by standard inversion recovery experiments.

RESULTS AND DISCUSSION

$Li_{2-x}Cu_xMgCl_4$ and $Li_{2-x}Na_xMgCl_4$ Spinel-Type Solid Solutions, Local Structure and Chemical Shifts of the Li^+ Ions

^{6}Li MAS NMR spectra of $Li_{2-x}Cu_xMgCl_4$ and $Li_{2-x}Na_xMgCl_4$ spinel-type solid solutions are shown in Fig. 1. The signals were analyzed with respect to intensities, half-widths, and shift parameters using standard curve fitting procedures. The results are given in Table 1. Due to the larger quadrupole moment of ^{7}Li as compared to ^{6}Li, the ^{7}Li MAS NMR signals display half-widths which exceed those of the ^{6}Li signals. In the case of ^{6}Li, at high spinning rates the whole intensity of the resonance is concentrated in the main signal and, hence, no rotational sidebands occur. This allowed satisfactory separation of chemically shifted signals. With respect to intensity measurements and the calculation of site occupation numbers, however, the long spin-lattice relaxation time of ^{6}Li found frequently is a drawback because systematic errors may be introduced due to incomplete relaxation. This possibility exists in the present case where signal 2 showed a T_1 of about 3×10^3 s (see below). The ^{7}Li T_1 values, on the other hand, are in order of ms (17), but here the stronger signal overlap may introduce integration errors. The changes of the relative intensities observed for the ^{6}Li signals, which we discuss below, however, are not affected by these shortcomings.

The ^{6}Li MAS NMR spectra of the spinel-type solid solutions under investigation are, in general, very similar to those of ternary Li_2MgCl_4 (7, 8). Thus, the chemical shifts δ of the two NMR signals 1 and 2, which we assign to the tetrahedral and the octahedral position, respectively (see below), are 1.2 and 0.2 ppm, as found for Li_2MgCl_4. These chemical shifts, however, do not change with decreasing lithium content in contrast to the behavior of $Li_{2-2x}Mg_{1+x}Cl_4$ solid solutions (7, 8). In the latter case, the high-field shift of the two signals observed with decreasing lithium content was ascribed to clustering of the lithium and magnesium ions in these metal ion deficient compounds (8). If this interpretation holds, the different behavior of the chemical shifts means that there is a random distribution of the sodium and copper ions at the respective lattice sites of the spinel-type solid solutions.

In some of the spectra, the line shape analysis revealed a third signal of low intensity and unknown origin with negligible chemical shift as compared to LiCl (Fig. 1 and Table 1). It is not clear at present if this represents a third site with low occupation or a minor impurity.

The intensity relations of the two NMR signals of the spinel-type solid solutions under investigation, however, differ from those of Li_2MgCl_4 and of $Li_{2-2x}Mg_{1+x}Cl_4$ solid solutions (7, 8) as expected. Thus, even if one considers the experimental uncertainties in the obtained data, in the case of the copper-containing compounds, the relative intensity

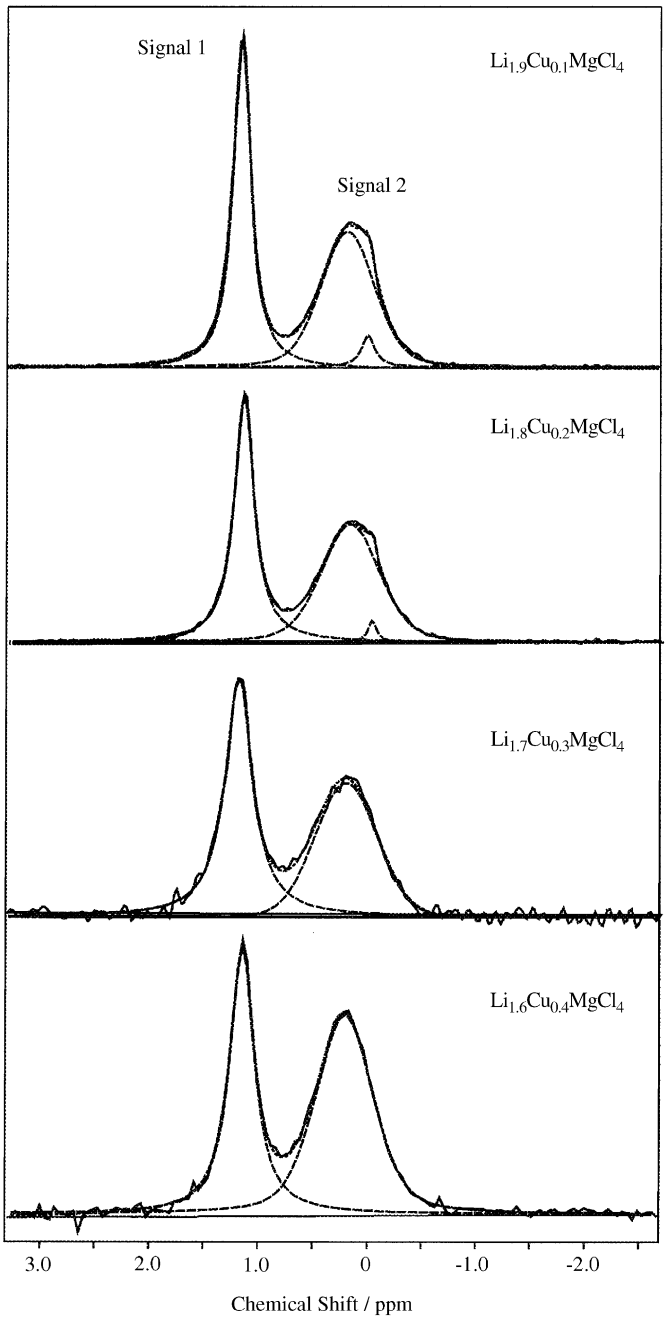

FIG. 1. ^{6}Li MAS NMR signals (spinning rate 10 kHz) of spinel-type $Li_{2-x}Cu_xMgCl_4$ solid solutions, fitted with combined Gaussian and Lorentz functions: ——, observed and ----, calculated profiles of the observed signals, respectively.

of the *low-field* signal 1 decreases with increasing copper content while the *high-field* signal 2 is not significantly affected (see Fig. 1 and Table 1). This confirms the assignment of the two main signals discussed before under the assumption that the Cu^+ ions solely replace the tetrahedral

TABLE 1

^{6}Li MAS NMR Data of Spinel-Type $Li_{2-x}Cu_xMgCl_4$ and $Li_{2-x}Na_xMgCl_4$ Solid Solutions (See Figs. 1 and 2); Data in Parentheses Are Due to a Small Third Signal (See Text)

	Signal 1 (tetrahedral, 8*a* site)			Signal 2 (octahedral, 16*d* site)		
Compounds	δ^a [ppm]	FWHM^b [Hz]	Int.^{c}	δ^a [ppm]	FWHM^b [Hz]	Int.^{b}
$^6Li_{1.9}Cu_{0.1}MgCl_4$	1.2	8.8	2.4	0.2	25.6	1.0
				(0.0)	(6.6)	(0.2)
$^6Li_{1.8}Cu_{0.2}MgCl_4$	1.2	9.7	2.1	0.2	27.4	1.0
				(0.0)	(4.4)	(0.2)
$^6Li_{1.7}Cu_{0.3}MgCl_4$	1.2	13.3	1.8	0.2	29.2	1.0
$^6Li_{1.6}Cu_{0.4}MgCl_4$	1.1	11.5	1.4	0.2	27.4	1.0
				(0.0)	(1.8)	(0.02)
$^6Li_{1.8}Na_{0.2}MgCl_4$	1.2	21.3	0.94	0.2	25.2	1.0
				(0.1)	(5.9)	(0.03)
$^6Li_{1.7}Na_{0.3}MgCl_4$	1.2	15.7	0.83	0.2	21.7	1.0

[a] Rel. to ext. solid LiCl.
[b] FWHM = signal width at half height.
[c] Intensity rel. to signal 2.

coordinated Li^+ ions in the inverse spinel structure of the $Li_{2-x}Cu_xMgCl_4$ solid solutions.

In the case of the $Li_{2-x}Na_xMgCl_4$ solid solutions again two signals are observed; however, the relative intensity of the *high-field* signal does not significantly decrease with increasing sodium content (see Fig. 2 and Table 1). This contradicts the results from neutron diffraction studies (12–14) which showed that octahedral coordinated Li^+ ions are replaced by Na^+. In addition, the preference of sodium ions for octahedral sites may also be deduced from the larger ionic radius of Na^+ as compared to that of Li^+. Further NMR measurements on these systems are, therefore, necessary to clarify this point.

SLOW MAS NMR Spectra of $Li_{2-x}Na_xMgCl_4$

It was of interest to determine the quadrupolar coupling constants (QCC) for the two lithium sites. For this purpose, we recorded slow MAS NMR spectra of $Li_{2-x}Na_xMgCl_4$ where this parameter can be determined by using the equation $QCC = 2I \times SW/3$ (18) with SW, the spectral width of the sidebands, and I, the nuclear spin quantum number. The ^{6}Li MAS NMR spectrum of $Li_{1.8}Na_{0.2}MgCl_4$ obtained with a rotational frequency of 507 Hz is shown in Fig. 3. Clearly, at such a low spinning rate the two ^{6}Li resonances are not more resolved but the asymmetric intensity distribution of the sidebands indicates the presence of a second Li signal with somewhat different quadrupole coupling constant, thus confirming the results of the fast MAS NMR experiments discussed above. Consequently, only the larger one of the two values expected for the different lithium

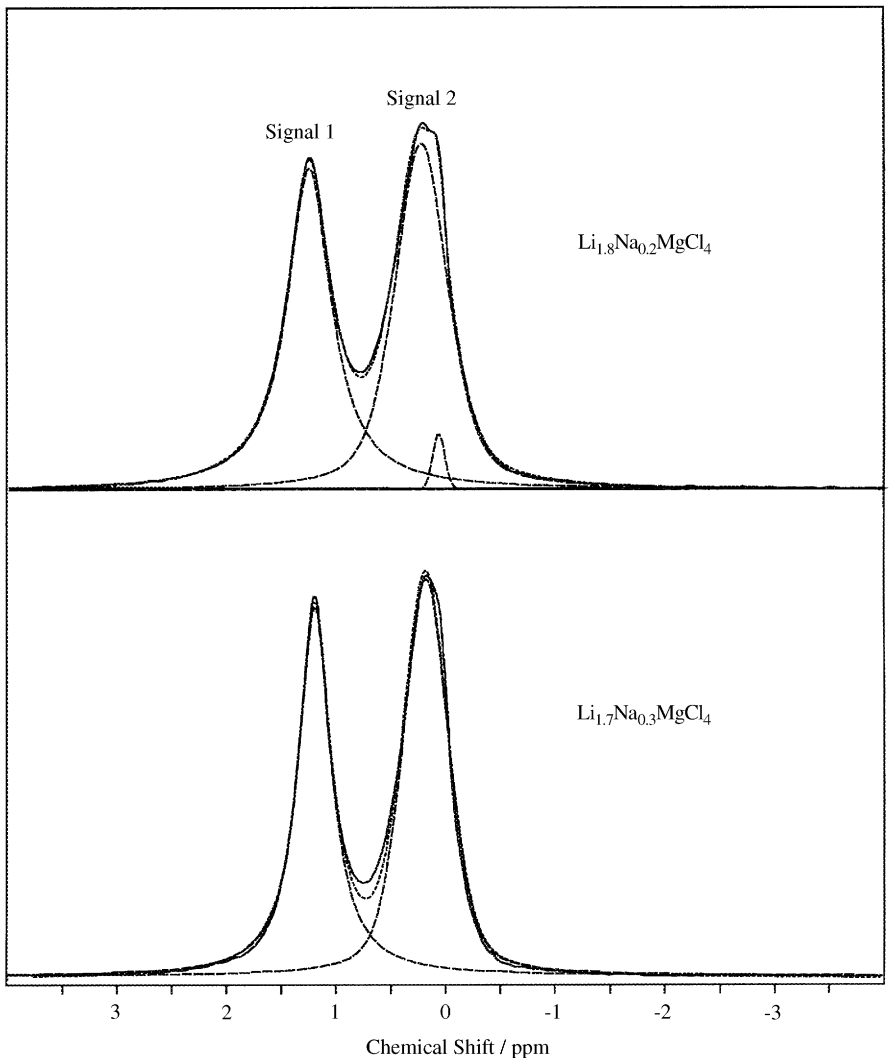

FIG. 2. ^{6}Li MAS NMR signals of spinel-type $Li_{2-x}Na_xMgCl_4$ solid solutions; for further explanations see Fig. 1.

positions of the inverse spinel structure, QCC_{max}, could be obtained from the sideband pattern. From the spectrum, we estimate a value of 4 kHz which corresponds to ca. 195 kHz for ^{7}Li according to the ratio of the respective quadrupolar moments [8.2/400 = 1/48.8 (19)]. This indicates a distorted octahedral and/or terahedral environment for Li^+ because otherwise the QCC should vanish. The direct measurement of QCC_{max} from the ^{7}Li slow MAS spectrum was not possible because of the low intensity of the outer sidebands which disappeared in the noise.

Temperature Dependence of the ^{6}Li MAS NMR Spectra of $Li_{2-x}Cu_xMgCl_4$

The temperature dependence of the ^{6}Li MAS NMR spectra of $Li_{1.8}Cu_{0.2}MgCl_4$ is shown in Fig. 4. It displays characteristic changes of intensities and half-widths of the two main signals and in addition small chemical shift changes. The most pronounced feature is the line-shape change of the low-field signal assigned to the tetrahedral site which sharpens around 233 K and broadens again around 313 K (Fig. 5). Consequently, it has an intensity maximum at ca. 273 K. This behavior points to the presence of a dynamic process.

The most interesting question with respect to the ion conductivity of $Li_{1.8}Cu_{0.2}MgCl_4$ is concerned with a possible chemical exchange process $Li^{tet} \Leftrightarrow Li^{oct}$. In this case, the observed spectra with two distinct resonances are characteristic for the slow exchange limit. Any shortening of the lifetime of the two states should lead to line broadening and eventually to the coalescence of the two signals. This is not observed. The decrease of the chemical shift difference with

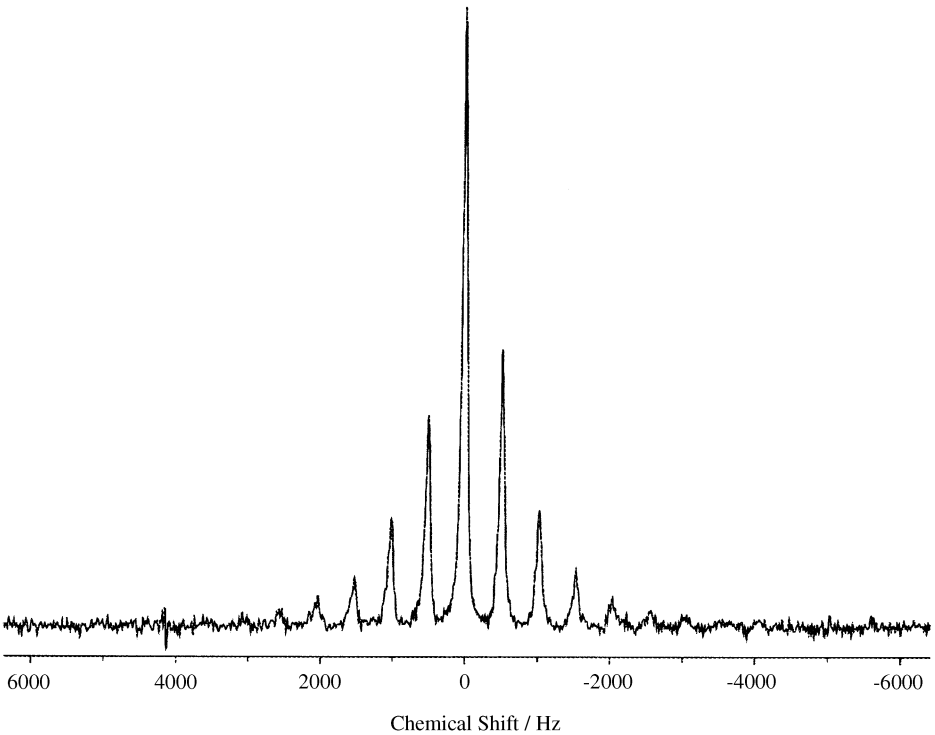

FIG. 3. ^{6}Li SLOW MAS NMR spectrum of spinel-type $Li_{1.8}Na_{0.2}MgCl_4$; spinning rate 507 s^{-1}.

the final overlap of the two signals at 373 K might suggest such a process; however, there is no line broadening involved and the merger of the two signals is not a true coalescence phenomenon but rather the consequence of the decrease in the chemical shift difference.

There is thus no clear indication of Li exchange. We can, however, estimate from the observed spectra the lower limit for the energy barrier of such a process. If we assume coalescence at the highest temperature reached (373 K), we derive with the simple relation

$$k = 2.22\ \Delta\nu, \qquad [1]$$

which holds for equally populated sites at the coalescence temperature (20) and the shift difference measured at 373 K (0.97 ppm or 43 Hz, see Table 1), a rate constant of $k(373) = 95$ and on the basis of the Eyring equation an activation energy of $\Delta G^*(373) = 79\ kJ\ mol^{-1}$. This means that a possible interchange of Li^+ cations between tetrahedral and octahedral sites is rather slow at temperatures below 400 K. The activation energy obtained is clearly in the range of the activation energy of the ionic conducting process at ambient temperature, viz., 75 kJ mol^{-1} (21–23), and of that derived from the ^{7}Li T_1 relaxation times of broadband NMR experiments of $^7Li_2MgCl_4$, viz., 71.4 kJ mol^{-1} (24). In the case of the latter experiments also, obviously the activation energy due to long-range diffusion processes of the Li ions has been established.

1D-EXSY Experiments on $^6Li_2MgCl_4$, Spin-Lattice Relaxation Time T_1 and Correlation Time τ_C of the Tetrahedral Coordinated Li^+ Ions

In order to investigate the temperature effect on the Li resonances of the spinel-type compounds in more detail, it was desirable to measure the individual relaxation times of Li^{tet} and Li^{oct}, respectively. For this purpose, we used selective 1D-EXSY experiments (16) for $^6Li_2MgCl_4$. They yield the individual spin-lattice relaxation times T_1 of the two sites as well as the rate constants for the chemical exchange between them. This method, which uses the pulse sequence $90_x - (t_1 = 1/\Delta\nu) - 90_x - \tau_M - 90_x$, FID, is applicable in case of slow chemical exchange and was applied here to the low-field signal. The interval t_1, which serves for the separation of the two signals and the selective inversion of the low-field signal, was adjusted at each temperature on the basis of the measured relative chemical shift, $\Delta\nu$ (in Hz), between the two sites. A typical set of spectra for a particular temperature is shown in Fig. 6. The spectra were analyzed on the basis of equation

$$M_{z,A}(\tau_M) = M_{z,A}(\infty)\left\{1 - \left(\frac{1+f}{2\beta}\right)\left[\left(\beta + \frac{1}{T_{1,A}} - \frac{1}{T_{1,B}}\right)e^{-1/2(\alpha+\beta)\tau_M} + \left(\beta + \frac{1}{T_{1,B}} - \frac{1}{T_{1,A}}\right)e^{-1/2(\alpha-\beta)\tau_M}\right]\right\} \qquad [2]$$

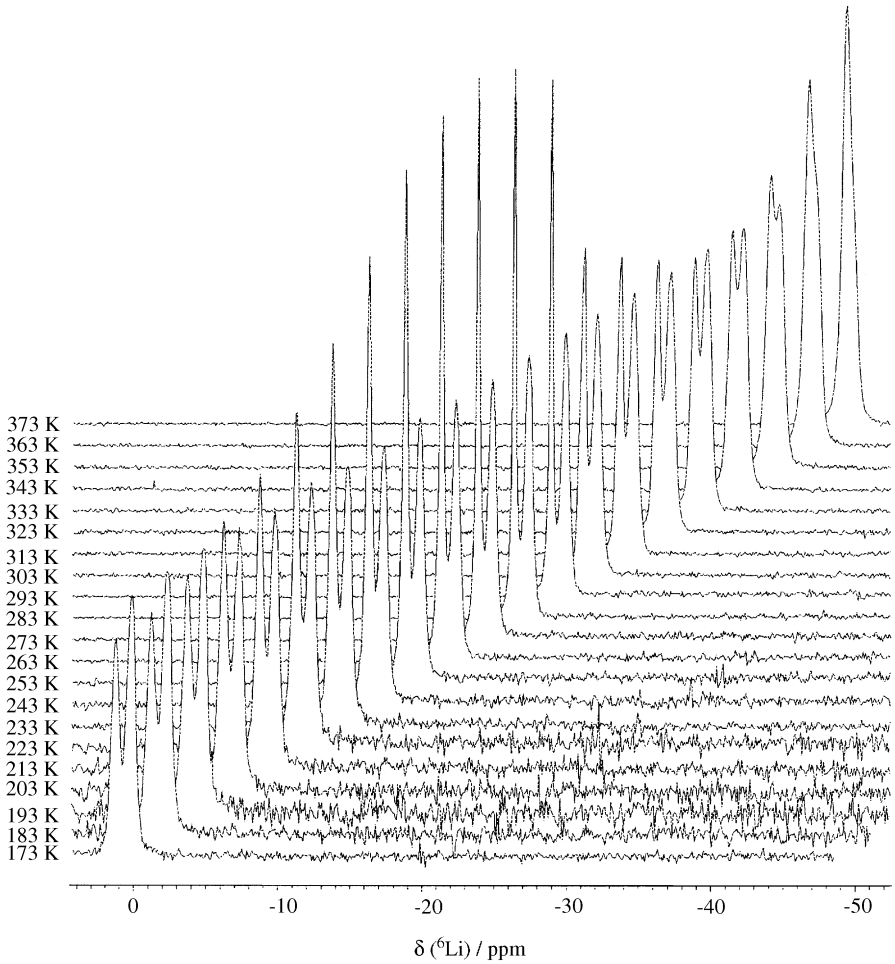

FIG. 4. Temperature dependence of the ^{6}Li MAS NMR spectra of spinel-type $Li_{1.8}Cu_{0.2}MgCl_4$ (stacked plot, the δ-scale only applies to the 173 K spectrum); the chemical shifts $\delta(^6Li)$ are 0.8, 0.3 ppm at 173 K and 1.2, 0.2 ppm at 353 K.

with

$$\alpha = 2k + \frac{1}{T_{1,\mathrm{B}}} + \frac{1}{T_{1,\mathrm{A}}} \quad \text{and} \quad \beta = \sqrt{\left(\frac{1}{T_{1,\mathrm{B}}} - \frac{1}{T_{1,\mathrm{A}}}\right)^2 + 4k^2},$$

where $M_{z,\mathrm{A}}(\infty)$ is the equilibrium magnetization of the inverted signal A, $T_{1,\mathrm{A}}$ is the longitudinal relaxation time of the inverted signal A, $T_{1,\mathrm{B}}$ is the longitudinal relaxation time of signal B, k is the rate constant for the process A↔B and f is a factor for incomplete inversion.

A typical result for the intensity of the low-field signal in relation to the mixing time τ_{M} is shown in Fig. 7 and the complete data are collected in Table 2. For the iterative analysis, the empirical inversion factor was set to 0.9 and the spin-lattice relaxation time of the high-field signal due to Li^{oct} was kept constant at 3187 s, a value which was consistently obtained in a number of trial fittings. The large value was later justified by separate measurements for $^6Li_2ZnCl_4$ (see below).

Significant changes for the rate constants were found only at the highest temperatures reached (Table 2), but the large experimental error for these data prevents an analysis on the basis of rate theory. It is interesting to note, however, that the measurements yielded at higher temperatures rate constants is in the order of that estimated above from the line shape behavior. This result thus independently supports the assumption of the existence of a slow exchange process of the type $Li^{tet} \Leftrightarrow Li^{oct}$ with a barrier $> 79\ \mathrm{kJ\,mol^{-1}}$.

The temperature dependence of the spin-lattice relaxation time for the Li^{tet} signal is shown in Fig. 8 and an Arrhenius plot of these data (Table 2) in Fig. 9. On the basis of a linear behavior of the low temperature data of up to 263 K, an Arrhenius activation energy E_a of 6.9 kJ mol^{-1} is obtained for the dynamic process that causes the variation in T_1 for the Li^{tet} signal (Figs. 8 and 9). Following the analysis applied by Emery *et al.* in a similar case we can derive on the basis of the Bloembergen–Purcell–Pound model (25) the correlation time for the motional process of the Li^+ cations in the

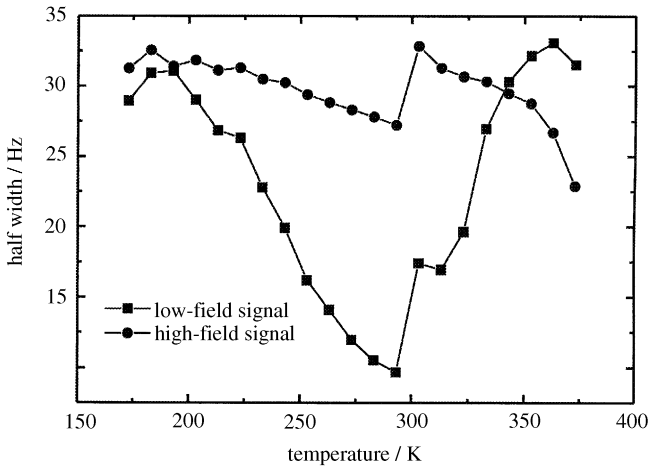

FIG. 5. Temperature dependence of the half-widths (FWHM) of the ^{6}Li MAS NMR signals of spinel-type $Li_{1.8}Cu_{0.2}MgCl_4$: ■, low-field signal; ●, high-field signal; exp. error ± 4 Hz.

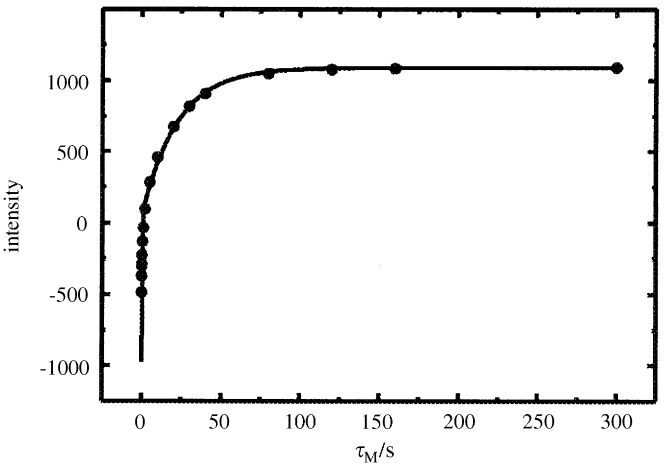

FIG. 7. Intensity of the low-field signal (Li^{tet}) of $^6Li_2MgCl_4$ at 283 K and various mixing times τ_M.

tetrahedral site on the basis of the following equation:

$$\frac{1}{T_1} = C\left[\frac{\tau_C}{1+(\omega_0\tau_C)} + \frac{4\tau_C}{1+(2\omega_0\tau_C)^2}\right], \qquad [3]$$

where $\omega_0\tau_C = 0.62$ (25) and ω_0/π is the ^{6}Li resonance frequency of 44.7 MHz. C is a constant which can be derived from the minimum of the T_1 curve which was assumed here at 343 K which yielded $C = 2.1 \times 10^7\ s^{-2}$. The correlation time τ_C was then derived for each temperature from equation

$$(4\omega_0^4)\tau_C^4 - (8\omega_0^2 T_1 C)\tau_C^3 + (5\omega_0^2)\tau_C^2 - (5T_1 C)\tau_C + 1 = 0\ . \qquad [4]$$

A plot of $\ln(1/\tau_C)$ against $1/T$ (data from Table 3) is shown in Fig. 10. The regression analysis yielded an activation

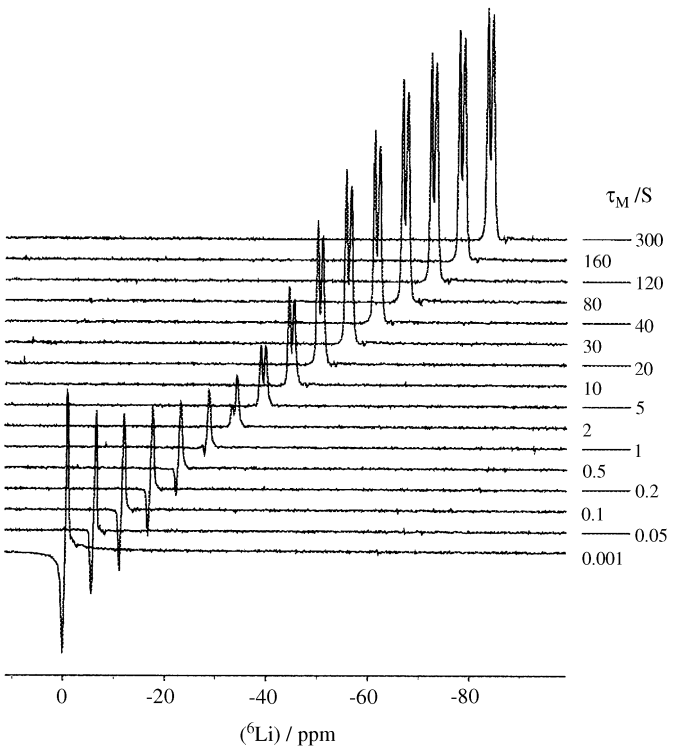

FIG. 6. ^{6}Li-1D-EXSY experiments of inverse spinel-type $^6Li_2MgCl_4$ at 283 K with selective inversion of the low-field signal at different mixing times τ_M.

TABLE 2

Spin-Lattice Relaxation Times T_{1A} of the Tetrahedral Coordinated Lithium Ions of Inverse Spinel-Type Li_2MgCl_4, Equilibrium Magnetization $M_{z,A(\infty)}$ of the Inverted Signal 1, and Reaction Rate k of the Site Exchange between Li^{tet} (8*a* Site) and Li_{oct} (16*d* Site) (See Figs. 6–8)

Temperature (K)	T_{1A} (s)	$M_{z,A}(\infty)$	k (s^{-1})
173	60.7 ± 14.8	921	1.0 ± 0.3
183	36.7 ± 12.1	841	1.5
193	35.0 ± 7.9	1061	0.3 ± 0.1
203	13.3 ± 3.0	835	1.8 ± 0.5
213	19.7 ± 4.4	1232	3.0 ± 0.8
223	18.4 ± 5.4	1209	0.5 ± 0.2
233	11.8 ± 2.1	1210	5.4 ± 1.2
243	9.4 ± 2.2	1181	0.2 ± 0.1
253	12.6 ± 5.6	1180	8.1 ± 4.8
263	12.5 ± 3.9	1205	3.1 ± 1.2
273	10.8 ± 2.1	1173	2.1 ± 0.5
283	11.2 ± 3.1	1090	11.7 ± 4.7
292	11.2 ± 2.9	3155	2.9 ± 0.9
293	11.2 ± 2.9	764	2.7 ± 0.9
303	11.1 ± 2.8	695	5.6 ± 1.7
313	11.1 ± 2.8	650	7.7 ± 2.6
323	9.8 ± 2.6	617	60.7 ± 29.0
333	10.2 ± 3.1	779	58.4 ± 32.3
343	9.3 ± 1.7	778	43.4 ± 14.1

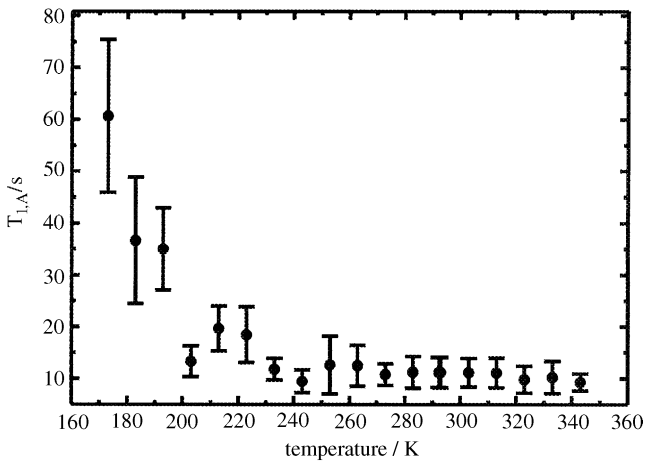

FIG. 8. Temperature evolution of the spin-lattice relaxation time T_{1A} of the tetrahedral coordinated lithium ions of spinel-type $^6Li_2MgCl_4$ (see Table 2).

TABLE 3
Correlation Times τ_C of the Tetrahedral Coordinated Lithium Ions of Inverse Spinel-Type Li_2MgCl_4 (See Fig. 10)

T (K)	$1/T/1000/K^{-1}$	$\tau_C/10^{-8}$ sec	$\ln(1/\tau_C)$
173	5.780	5.89	16.65
183	5.464	1.95	17.75
193	5.181	1.86	17.80
203	4.926	0.60	18.94
213	4.695	0.99	18.43
223	4.484	0.92	18.51
233	4.292	0.49	19.13
243	4.115	0.26	19.76
253	3.952	0.55	19.02
263	3.802	0.54	19.04
273	3.663	0.41	19.30
283	3.533	0.45	19.23
292.4	3.420	0.45	19.23
293	3.413	0.45	19.23
303	3.300	0.44	19.25
313	3.195	0.44	19.25
323	3.096	0.32	19.56
333	3.003	0.36	19.44
343	2.015	0.22	19.92

energy E_a of 6.6 kJ/mol^{-1} or 0.07 eV in excellent agreement with the value derived above.

The spin-lattice relaxation time of the octahedral coordinated lithium ions T_{1B} is much larger than T_{1A} (see also below). This means that the motion of the octahedral coordinated lithium ions of Li_2MgCl_4 is much slower than that of the tetrahedral coordinated ones as already established by conductivity (3, 5) and quasielastic neutron scattering experiments (26). The activation energies obtained from the 1D-EXSY experiments on the low-field signal of Li_2MgCl_4 (6.9 and 6.6 kJ mol^{-1}) also differ from the activation energy of 23 kJ mol^{-1} (26) derived via quasielastic neutron scattering experiments. The latter energy has been ascribed to local motions of the tetrahedral coordinated Li^+ ions from 8*a* lattice sites to 16*c* interstitial sites and backwards. Hence, the lower activation energy obtained by the NMR experiments may be due to local motions of the tetrahedral coordinated Li^+ ions inside the respective lattice site. This may mean that the real lattice site of Li^{tet} in spinel-type ternary chlorides is not 8*a* but 32*e* (occupation factor 0.25) with one somewhat shorter and three somewhat longer Li–Cl distances. In cubic close packed chlorides, the tetrahedral voids are larger than needed for Li^+ ions as already discussed in

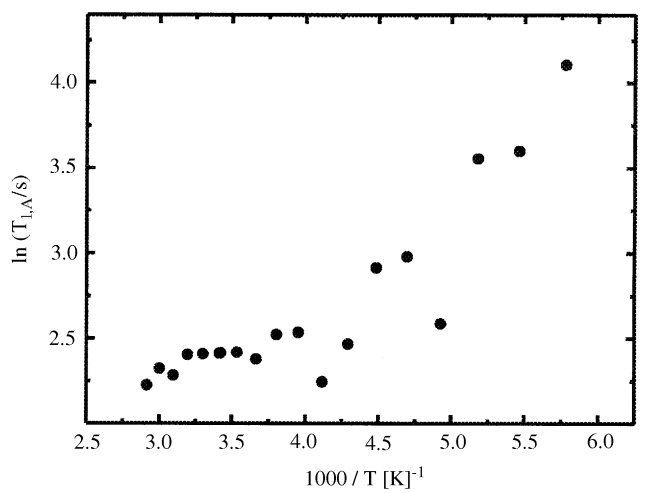

FIG. 9. Arrhenius plot of the spin-lattice relaxation time T_{1A} of the tetrahedral coordinated lithium ions of $^6Li_2MgCl_4$ (see Table 2).

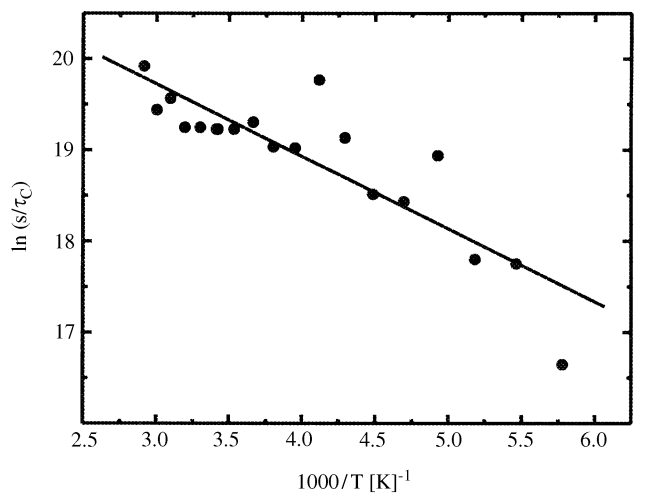

FIG. 10. Arrhenius plot of the correlation times τ_C of the tetrahedral coordinated lithium ions of $^6Li_2MgCl_4$ (see Table 3).

(10). Hence, the dynamic process under discussion may be due to Li ions hopping between 32*e* sites.

Inversion Recovery Experiments on $^6Li_2ZnCl_4$, Relaxation Time T_1 of Octahedral Coordinated Li^+ Ions

As described above, the EXSY experiments yielded a rather long spin-lattice relaxation time for the high-field signal due to the octahedral site which was kept constant to facilitate the fitting of the experimental data. In order to independently support this result, we performed inversion recovery experiments on $^6Li_2ZnCl_4$ (11). In this compound, the lithium ions are solely placed at octahedral sites of normal spinel-type structure of this ternary chloride. Standard inversion recovery experiments for the ^{6}Li signal gave a T_1 value of ca. 3×10^3 s which compares favorably with the value obtained above for $^6Li_2MgCl_4$. The uncertainty is a consequence of the fact that for obvious reasons the delay time had to be shorter than the required $5T_1$. However, if we take the result as a measure of the relaxation time T_{1B} of the octahedral coordinated Li^+ ions of inverse spinel-type ternary lithium chlorides as Li_2MgCl_4, the spin-lattice relaxation time of these Li^+ ions is much longer than that of the tetrahedral coordinated Li^+ ions. Hence, the local mobility of Li^{oct} is lower than that of Li^{tet}.

CONCLUSION

In the case of fast ionic conducting ternary lithium chlorides with inverse spinel-type structure, activation energies ΔG^* of five different dynamic processes, viz., 23, 29, 75, and >79 kJ mol^{-1}, have been established. The interchange of the lithium ions between the tetrahedral and octahedral sites of the crystal structure is very slow with $\Delta G^* > 79$ kJ mol^{-1}. The long-range ionic conducting process of the tetrahedral coordinated Li^+ ions via empty octahedral 16*c* sites (3) is associated with $\Delta G^* = 75$ kJ mol^{-1} at ambient and 29 kJ mol^{-1} at elevated temperatures, respectively (23). The smaller ΔG^* above ca. 600 K (21, 23) is due to long-range hopping of Li^+ ions disordered between the tetrahedral 8*a* sites and octahedral 16*c* interstitial sites (5), the higher ΔG^* below 600 K includes the free energy necessary for the formation of the respective Frenkel defects, i.e., 16*c* interstitial Li^+ ions. The energy barrier $\Delta G^* = 23$ kJ mol^{-1} is due to the relatively rapid local motions of the Li ions between the tetrahedral 8*a* and the octahedral interstitial 16*c* sites (26, 27). Finally, there are very rapid hopping motions of the lithium ions between 32*e* split sites inside the tetrahedral voids of cubic close packing of the Cl^- ions with $E_a = 6.6$–6.9 kJ mol^{-1}. In the $Li_{2-x}Cu_xMgCl_4$ and $Li_{2-x}Na_xMgCl_4$ spinel-type solid solutions studied, the copper(I) and sodium ions are randomly distributed on the tetrahedral 8*a* and the octahedral 16*d* sites, respectively, in contrast to deficient spinel-type $Li_{2-2x}Mg_{1+x}Cl_4$ solid solutions with clustering of the Mg^{2+} ions around the vacancies.

ACKNOWLEDGMENTS

We are indebted to Dr. M. Hartung for initial measurements and to the VW Stiftung for a spectrometer grant.

REFERENCES

1. R. Kanno, Y. Takeda, K. Takada, and O. Yamamoto, *J. Electrochem. Soc.* **131,** 469 (1984).
2. H. D. Lutz, *Nachr. Chem. Tech. Lab.* **43,** 418 (1995).
3. H. D. Lutz, P. Kuske, and K. Wussow, *Solid State Ionics* **28–30,** 1282 (1988).
4. A. West, *Ber. Bunsenges. Phys. Chem.* **93,** 1235 (1989).
5. (a) H.-J. Steiner and H. D. Lutz, *J. Solid State Chem.* **99,** 1 (1992); (b) Ch. Wickel and H. D. Lutz, *Z. Kristallogr. NCS.* **213,** 27 (1998).
6. P. Kuske, W. Schäfer, and H. D. Lutz, *Mater. Res. Bull.* **23,** 1805 (1988).
7. Ch. Wickel, J. Senker, and H. D. Lutz, *Cryst. Res. Technol.* **31,** 881 (1996).
8. R. Nagel, Ch. Wickel, J. Senker, and H. D. Lutz, *Solid State Ionics* **130,** 169 (2000).
9. R. Kanno, O Yamamoto, Ch. Cros, and J. L. Soubeyroux, *Nato ASI Ser., Ser. E* **101,** 460 (1985).
10. Ch. Wickel, Z. Zhang, and H. D. Lutz, *Z. Anorg. Allg. Chem.* **620,** 1537 (1994).
11. Th. W. Groß, Doctoral Thesis, University of Siegen, 1999.
12. R. Nagel, Doctoral Thesis, University of Siegen, 2001.
13. H. D. Lutz, P. Kuske, and A. Pfitzner, *Ber. Bunsenges. Phys. Chem.* **93,** 1340 (1989).
14. R. Nagel and H. D. Lutz (in preparation).
15. DISMSL, Version 911101.1, © Bruker-Franzen Analytische Messtechnik GmbH, 1991.
16. G. A. Morris and R. Freeman, *J. Magn. Reson.* **29,** 433 (1978).
17. J. Emery, J. Y. Buzare, O. Bohnke, and J. L. Fourquet, *Solid State Ionics* **99,** 41 (1997).
18. (a) J. P. Amoureux, C. Fernandéz, and P. Granger, NATO ASI Series—Series C, **322,** 409 (1990); (b) J. Skibsted, N. C. Nielsen, H. Bildsöe, and H. J. Jakobsen, *J. Magn. Reson.* **42,** 88 (1991).
19. R. K. Harris, *in* "Encyclopedia of NMR" (D. M. Grant and R. K. Harris, Eds), Vol. 5, p. 3301. Wiley, Chichester, 1996.
20. H. Günther, "NMR Spectroscopy," Chapter 9. Wiley, New York, 1998.
21. H. D. Lutz, W. Schmidt, and H. Haeuseler, *J. Phys. Chem. Solids* **81,** 287 (1981).
22. R. Kanno, Y. Takeda, and O Yamamoto, *Mater. Res. Bull.* **16,** 999 (1981).
23. H. D. Lutz, A. Pfitzner, and I. Solinas, *Solid State Ionics* **52,** 353 (1992).
24. J. Spector, G. Villeneuve, L. Hanebali, and Ch. Cros, *Mater. Lett.* **1,** 43 (1982).
25. N. Bloembergen, E. M. Purcell, and R. V. Pound, *Phys. Rev.* **73,** 679 (1948).
26. G. A. Eckstein, G. Eckold, W. Schmidt, H.-J. Steiner, and H. D. Lutz, *Solid State Ionics* **111,** 283 (1998).
27. M. Partik, M. Schneider, and H. D. Lutz, *Z. Anorg. Allg. Chem.* **620,** 791 (1994).